

Interaction between Polymer-Grafted Particles

Jaep U. Kim^{*,†} and Mark W. Matsen^{*,‡}

Department of Mathematics, University of Reading, Whiteknights, Reading RG6 6AX, U.K.

Received February 7, 2008; Revised Manuscript Received March 7, 2008

ABSTRACT: Previous self-consistent field theory (SCFT) calculations have predicted that the steric interaction between two polymer-grafted particles in good solvent can become attractive, but this conclusion has since been questioned. Here we reexamine the problem with a new numerical scheme using multiple coordinate systems, and find that the interaction remains repulsive regardless of the particle size, brush thickness, or particle separation. The erroneous attraction in the earlier calculations can be attributed to numerical inaccuracy and a subtle issue with how the chains were grafted to the particles. Using our corrected SCFT solution, we also investigate the accuracy of a previous calculation based on strong-stretching theory (SST) and the applicability of the Derjaguin approximation, where the interaction between large particles is estimated from the one-dimensional uniform compression of polymer brushes.

Introduction

The grafting of polymer chains to particles, as illustrated in Figure 1, is a well established method of stabilizing colloidal suspensions.¹ The polymeric brush provides a steric repulsion that helps disperse the colloids countering their tendency to aggregate due to van der Waals attraction. Theoretical treatments for the repulsion between two particles have generally been based on the Derjaguin approximation,² where the force is approximated in terms of simple uniform compression. This should provide a good estimate when the particles are much larger than the brush thickness, which is typically the case for colloidal suspensions. However, in this new era of nanotechnology, applications such as drug delivery are emerging where the particles are now much smaller.³

When the particle size becomes comparable to the brush thickness, the standard Derjaguin-type calculation significantly overestimates the range of the interaction, because it ignores the reduction in the brush thickness due to the curvature of the grafting surface. Even when modified to include this effect, it still neglects the fact that the polymer chains can escape from the gap between the particles by a simple lateral displacement (or tilting). These issues are well demonstrated in ref 4 using a semianalytical calculation based on the strong-stretching theory (SST) of Semenov⁵ and Milner et al.⁶ However, this treatment is not expected to be particularly accurate, because its strong-stretching assumption is rather unrealistic.⁷ Of course, more accurate predictions can be obtained with Monte Carlo simulations,^{8,9} but the high computational demands of this approach limit its applicability to short polymers and low grafting densities. In addition, simulations are generally performed in a vacuum using polymer chains composed of inert hard-sphere monomers, which further limits their applicability to Θ solvents.

A potentially less computational but still reasonably accurate approach is to use the numerical self-consistent field theory (SCFT). Although it retains the mean-field approximation used by SST, it removes the strong-stretching assumption. Wijmans and co-workers¹⁰ performed the first such calculation for athermal solvents by implementing a lattice version of SCFT¹¹ in a cylindrical coordinate system. Although they nicely demonstrated significant deviations from the Derjaguin approximation, their approach constrains the

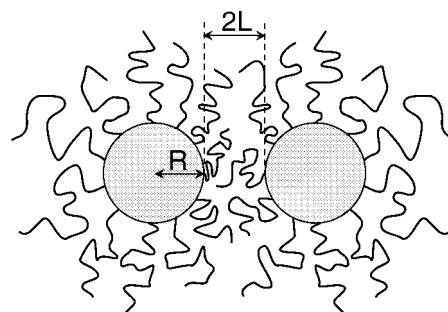


Figure 1. Schematic diagram of two spherical polymer-grafted particles of radius, R , separated by a distance, $2L$.

polymers to an artificial lattice and the calculation becomes computationally demanding for high molecular weights or large particles. More recently, Roan^{12,13} has performed calculations for good solvents with the more elegant continuum SCFT¹⁴ in a bispherical coordinate system.^{15,16} Interestingly, he found that for sufficiently small particles the interaction potential becomes negative (relative to infinite separation), which of course implies an attraction. However, it has been argued¹⁷ on theoretical grounds that the potential must remain positive within the mean-field approximation. This suggests that the SCFT calculation was not performed with sufficient numerical accuracy on account of the high computational demands of working with bispherical coordinates. Although subsequent Monte Carlo simulations and density-functional theory⁸ provide further evidence against the attraction, they do not actually test the SCFT prediction using the same model or even equivalent solvent conditions; thus, the controversy remains unresolved.

Here we develop a new numerical scheme, where the exact same SCFT is solved using multiple coordinate systems. By replacing the complex bispherical coordinate system with separate spherical-polar coordinate systems centered on each particle, the computational demands of the calculation are vastly reduced allowing us to eliminate any significant numerical inaccuracy. As expected, we find that the force between the two particles is purely repulsive regardless of the particle size, brush thickness, or particle separation. We also take advantage of our full SCFT solution to examine the accuracy of the former SST approach in ref 4 and to test the reliability of the Derjaguin approximation.

* Corresponding authors.

[†] E-mail: j.kim@reading.ac.uk.

[‡] E-mail: m.w.matsen@reading.ac.uk.

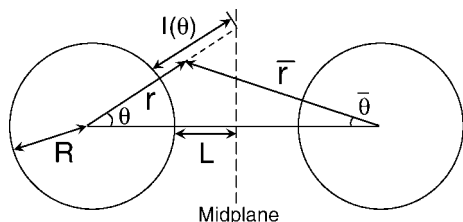


Figure 2. Multicoordinate-system (MCS) scheme, which makes use of two spherical-polar coordinate systems, one where points are specified from the center of particle one by $\mathbf{r} = (r, \theta, \varphi)$ and another where they are specified from the center of particle two by $\bar{\mathbf{r}} = (\bar{r}, \bar{\theta}, \bar{\varphi})$. In the case of identical particles, the interaction can be estimated with the Derjaguin approximation by assuming the brush at each angle θ is uniformly compressed to a thickness of $l(\theta)$.

Theory

This section presents the self-consistent field theory (SCFT) for two identical particles, each of radius R with n end-grafted polymer chains, separated by a distance $2L$ in a good solvent background (see Figure 1). Most of our calculations will assume a fixed uniform grafting density, $\sigma \equiv n/\mathcal{A}$, but we will also perform some calculations where the chain ends are free to move over the grafting area, \mathcal{A} , of each particle. The polymers will be treated as Gaussian chains, each with a natural end-to-end length of $aN^{1/2}$, where a is the statistical segment length and N is the number of segments per chain. To specify the course-grained trajectory of the α th chain, we define the space curve, $\mathbf{r}_\alpha(s)$, where the parameter s increases along the polymer backbone from 0 at the free end to 1 at the grafted end. The concentration of the first n polymers grafted to particle one can then be specified as

$$\hat{\phi}_1(\mathbf{r}) = \frac{N}{\rho_0} \sum_{\alpha=1}^n \int_0^1 ds \delta(\mathbf{r} - \mathbf{r}_\alpha(s)) \quad (1)$$

where ρ_0^{-1} is the segment volume. The concentration of the polymers grafted to particle two, $\hat{\phi}_2(\mathbf{r})$, is given by the same expression but with $\alpha = (n + 1)$ to $2n$. For computational reasons that will soon become obvious, the chains are grafted an infinitesimal distance, ε , above the particle surface such that the grafting area is $\mathcal{A} = 4\pi(R + \varepsilon)^2$.

The SCFT approximates the energy of each chain by

$$\frac{E[\mathbf{r}_\alpha]}{k_B T} = \int_0^1 ds \left(\frac{3}{2a^2 N} \left| \frac{d}{ds} \mathbf{r}_\alpha(s) \right|^2 + w(\mathbf{r}_\alpha(s)) \right) \quad (2)$$

where the first term is the entropic energy due to the multiple polymer configurations conforming to a given course-grained path, $\mathbf{r}_\alpha(s)$,¹⁸ and the second term involves a mean field, $w(\mathbf{r})$, representing the solvent–polymer interactions and the translational entropy of the solvent,⁷ which is treated implicitly. The field can be approximated by

$$w(\mathbf{r}) = \nu N (\hat{\phi}_1(\mathbf{r}) + \hat{\phi}_2(\mathbf{r})) \quad (3)$$

provided that ν , referred to as the excluded-volume parameter, is large enough to maintain a low segment density (i.e., the semidilute regime).^{6,7} Because we wish to focus solely on the steric interaction created by the brushes, the particles are treated as inert objects without any van der Waals interaction and without any surface affinity for either the polymer or the solvent. If need be, these interactions can easily be incorporated into the theory, but of course that would introduce additional parameters to contend with.

If at all possible, we would rather reduce the number of system parameters. Fortunately, in mean-field theory, the molecular weight dependence, N , can be scaled out of the problem by dividing all lengths (e.g., R and L) by $aN^{1/2}$ and by

multiplying all interaction parameters (e.g., ν) by N . Furthermore, in the semidilute limit, the grafting density, σ , can also be scaled out of the problem by defining the average concentration as^{7,19}

$$\phi_1(\mathbf{r}) = \frac{a\rho_0}{\sigma N^{1/2}} \langle \hat{\phi}_1(\mathbf{r}) \rangle \quad (4)$$

normalized such that

$$\int d\mathbf{r} \phi_1(\mathbf{r}) = \mathcal{A} a N^{1/2} \quad (5)$$

This allows the field, eq 3, to be rewritten as

$$w(\mathbf{r}) = \Lambda (\phi_1(\mathbf{r}) + \phi_2(\mathbf{r})) \quad (6)$$

where

$$\Lambda \equiv \frac{\nu \sigma N^{3/2}}{a\rho_0} \quad (7)$$

is now the only parameter controlling the extension of the polymer brush. Note that we will follow the common practice of specifying Λ by the more intuitive quantity,

$$\frac{L_0}{aN^{1/2}} = \left(\frac{4\Lambda}{\pi^2} \right)^{1/3} \quad (8)$$

which is the SST prediction for the height of a flat brush relative to the natural end-to-end length of a single chain.^{6,7} It should be mentioned that this ratio loses some of its relevance when dealing with spherical particles, because the height of a curved brush, L_B , decreases with increasing curvature. Nevertheless, $L_B/aN^{1/2}$ for a given $R/aN^{1/2}$ can be easily estimated from $L_0/aN^{1/2}$, using the simple algebraic equation derived in the Appendix (see eq 29).

To calculate $\phi_1(\mathbf{r})$, it is most convenient to work in a spherical–polar coordinate system, $\mathbf{r} = (r, \theta, \varphi)$, with the origin centered on particle one and the $\theta = 0$ direction oriented toward the center of particle two. Even though the second particle breaks the symmetry in the θ direction, the problem remains a relatively simple two-dimensional calculation because of the angular symmetry in φ . Once we know the polymer concentration from particle one, the mirror symmetry in Figure 2 implies that the concentration from particle two is

$$\phi_2(\mathbf{r}) = \phi_1(\bar{\mathbf{r}}) \quad (9)$$

where $\bar{\mathbf{r}} = (\bar{r}, \bar{\theta}, \bar{\varphi})$ corresponds to a spherical-polar system centered on particle two. The $\bar{\mathbf{r}}$ for a given \mathbf{r} is provided by the transformation

$$\bar{r} = \sqrt{r^2 + 4(R+L)^2 - 4r(R+L)\cos\theta} \quad (10)$$

$$\bar{\theta} = \tan^{-1} \left(\frac{r \sin\theta}{2(R+L) - r \cos\theta} \right) \quad (11)$$

$$\bar{\varphi} = \varphi \quad (12)$$

The SCFT for brushes with a fixed uniform grafting density, characteristic of covalently bonded chains,¹³ is derived in ref 19. As usual, the polymer concentration,

$$\phi_1(\mathbf{r}) = \int_0^1 ds q_f(\mathbf{r}, s) q_g(\mathbf{r}, 1-s) \quad (13)$$

and the free chain end distribution

$$g_1(\mathbf{r}) = q_g(\mathbf{r}, 1) \quad (14)$$

of particle one are expressed in terms of two partial partition functions, one for each end of a polymer chain. Both functions satisfy the same diffusion equation,¹⁸

$$\frac{\partial}{\partial s} q(\mathbf{r}, s) = \left[\frac{a^2 N}{6} \nabla^2 - w(\mathbf{r}) \right] q(\mathbf{r}, s) \quad (15)$$

where the impenetrability of the particles is accounted for by enforcing the Dirichlet boundary condition, $q(\mathbf{r}, s) = 0$, at $r = R$ and $\bar{r} = R$. The difference in the two functions is that $q_f(\mathbf{r}, s)$ for the free end of the chain satisfies the initial condition

$$q_f(\mathbf{r}, 0) = 1 \quad (16)$$

whereas $q_g(\mathbf{r}, s)$ for the grafted end satisfies

$$q_g(\mathbf{r}, 0) = \frac{\delta(r - R - \varepsilon) a N^{1/2}}{q_f(\mathbf{r}, 1)} \quad (17)$$

Note that the delta function actually bonds the chain ends slightly above the particle at $r = R + \varepsilon$, because otherwise $q_g(\mathbf{r}, 0)$ would violate the Dirichlet boundary condition.

The next step after calculating the total concentration, $\phi(\mathbf{r}) = \phi_1(\mathbf{r}) + \phi_2(\mathbf{r})$, is to adjust the field, $w(\mathbf{r})$, so as to satisfy eq 6. Once this is done, the free energy of particle one is evaluated by

$$\frac{F(L; R)}{k_B T} = -\sigma \int d\mathbf{r} \delta(r - R - \varepsilon) \ln q_f(\mathbf{r}, 1) - \frac{\sigma}{2a N^{1/2}} \int d\mathbf{r} w(\mathbf{r}) \phi_1(\mathbf{r}) \quad (18)$$

The first term integrates the single-chain free energy, $-k_B T \ln q_f(\mathbf{r}, 1)$, over the grafting surface, $r = R + \varepsilon$, while the second term corrects for the fact that mean-field theory double counts the internal energy. Of course, the free energy of particle two is identical by symmetry.

If the chain ends are only physically adsorbed and are free to move over the particle surface,¹² the SCFT equations remain the same except for the initial condition in eq 17, which is replaced by

$$q_g(\mathbf{r}, 0) \equiv \frac{\mathcal{A} \delta(r - R - \varepsilon) a N^{1/2}}{\int d\mathbf{r}' \delta(r' - R - \varepsilon) q_f(\mathbf{r}', 1)} \quad (19)$$

and the free energy in eq 18, which becomes

$$\frac{F(L; R)}{k_B T} = -\sigma \mathcal{A} \ln \left(\frac{1}{\mathcal{A}} \int d\mathbf{r} \delta(r - R - \varepsilon) q_f(\mathbf{r}, 1) \right) - \frac{\sigma}{2a N^{1/2}} \int d\mathbf{r} w(\mathbf{r}) \phi_1(\mathbf{r}) \quad (20)$$

With this modification, the grafted ends adopt the equilibrium distribution,

$$\sigma(\theta) = \frac{4\pi\sigma}{\mathcal{A} a N^{1/2}} \int_R^\infty dr r^2 q_f(r, \theta, 1) q_g(r, \theta, 0) \quad (21)$$

Notice that if the previous initial condition in eq 17 is used for $q_g(r, \theta, 0)$, the above distribution reduces to $\sigma(\theta) = \sigma$ as required.

To solve the equations of SCFT, we follow the usual approach of representing continuous space by a discrete grid, but with a mesh spacing that is generally an order of magnitude finer than in previous calculations.^{10,20} For particle one, the mesh has a regular spacing of $\Delta\theta = 0.0025\pi$ for $\theta = 0$ to π and a spacing of $\Delta r = 0.01a N^{1/2}$ for $r = R$ to $R + R_{\max}$. The value of R_{\max} is always chosen sufficiently large that $\phi_1(\mathbf{r}) < 10^{-9}$ on the outer boundary. For particle two, there is an equivalent mesh defined for the coordinates, $\bar{\mathbf{r}}$. Naturally, the grid points of the two coordinate systems will not exactly coincide, but nevertheless the transformation between them in eqs 10–12 is easily performed by using linear interpolation. To solve the diffusion equation (see eq 15), we use the Crank–Nicholson algorithm with small *time-steps* of $\Delta s = 0.00125$. In the initial condition

for $q_g(r, \theta, 0)$, we set the grafting surface at the first mesh point above the particle surface (i.e., $\varepsilon = \Delta r$). To maximize stability and computational efficiency, the alternating-direction implicit (ADI) scheme²¹ is used, where a half-time-step is performed treating θ implicitly and r explicitly and then vice versa for the next half-time-step. To help maintain the conservation of polymer, we previously found¹⁹ that it is best to only apply the field, $w(\mathbf{r})$, at integer time-steps rather than splitting it with the half-integer time-steps. The conservation is also improved by evaluating the volume integrals, $\int d\mathbf{r} f(\mathbf{r})$, using a simple quadrature where the integrand, $f(r, \theta)$, at each grid point is weighted by the volume of its own cell, defined as the region of space closest to that particular grid point. The self-consistent field eq 6 is satisfied using a simple iterative scheme, where the $(n + 1)$ th estimate, $w_{\text{in}}^{n+1} = (1 - \lambda)w_{\text{in}}^n + \lambda w_{\text{out}}^n$, is a mixture of the input field, w_{in}^n , and the output field, $w_{\text{out}}^n \equiv \Lambda\phi$, with a sufficiently small mixing ratio, $\lambda \approx 0.1$, to ensure convergence. We also apply Anderson-mixing²² every 10th step, which speeds up the convergence by a factor of about 5. For a given set of parameters (e.g., R , L_0 , and L), an accurate solution takes no more than 1 h running as a serial job on a 2.4 GHz AMD Opteron CPU.

Derjaguin Approximation

The Derjaguin approximation² is commonly used to estimate the two-particle interaction energy in terms of uniform compression. The most accurate approach^{4,23} uses the free energy per chain, $f(l; R)$, from a single particle of radius, R , with its brush compressed to a thickness of l . The Appendix provides a simple analytical estimate for $f(l; R)$ calculated with SST. In SCFT, $f(l; R)$ has to be evaluated numerically, but this is nevertheless a trivial one-dimensional calculation of an isolated particle with a reflecting boundary placed at $r = R + l$. Once the free energy of the uniformly compressed brush is known, the interaction energy of nonuniform compression is approximated as

$$\Delta F(L; R) = \sigma \int_0^\pi d\theta 2\pi R^2 \sin \theta \Delta f(l(\theta); R) \quad (22)$$

where $\Delta f(l; R) \equiv f(l; R) - f(\infty; R)$ and

$$l(\theta) = \frac{L + R}{\cos \theta} - R \quad (23)$$

is the distance from the particle surface to the midplane at the given angle (see Figure 2). The expression can be simplified to

$$\Delta F(L; R) = 2\pi\sigma R^2 (R + L) \int_L^\infty dl \frac{\Delta f(l; R)}{(R + l)^2} \quad (24)$$

by performing a change of variable from θ to l .

Although eq 24 already represents a relatively easy calculation, the standard Derjaguin approach goes a step further by taking the limit of large R , in which case the expression reduces to^{10,24}

$$\Delta F(L; R) = 2\pi\sigma R \int_L^\infty dl \Delta f(l; \infty) \quad (25)$$

Not only does this form predict a simple linear dependence on the particle radius, R , but also the force on each particle

$$\text{force} \equiv -\frac{d}{dL} \Delta F(L; R) = 2\pi\sigma R \Delta f(L; \infty) \quad (26)$$

only requires the calculation of $f(l; R)$ for a flat brush, $R \rightarrow \infty$, compressed to a single thickness of $l = L$. The drawback, however, is that the approximation will breakdown more quickly as R decreases.

Results

The range of the particle–particle interaction is naturally determined by the unperturbed thickness of the polymer brush, and therefore we begin by examining an isolated particle (i.e.,

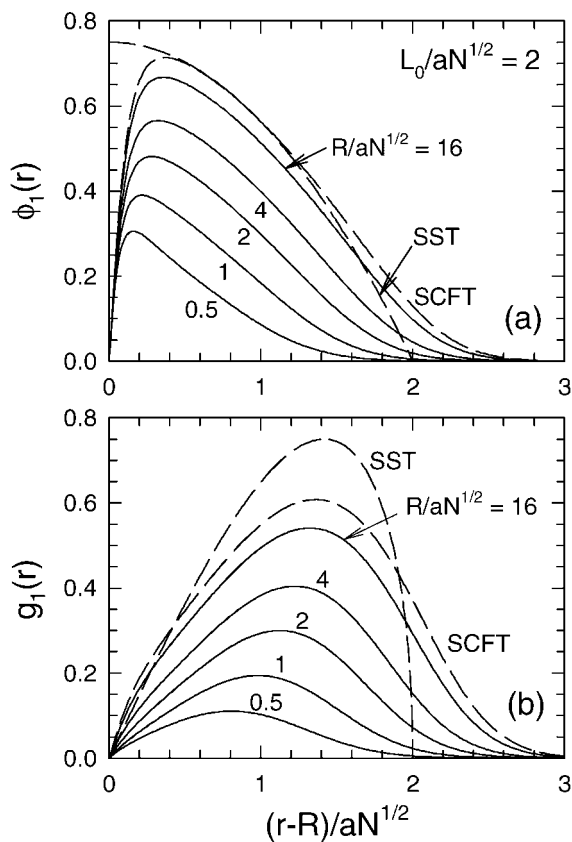


Figure 3. (a) Polymer concentration, $\phi_1(r)$, and (b) end-segment distribution, $g_1(r)$, of isolated particles with various radii, R , and a fixed Λ corresponding to $L_0 = 2aN^{1/2}$. The flat brush limits ($R \rightarrow \infty$) of SCFT and SST are denoted with dashed curves.

$L \rightarrow \infty$).²⁵ Figure 3 shows the profile, $\phi_1(r)$, and end-segment distribution, $g_1(r)$, for a series of different particle radii, R , at a fixed Λ corresponding to $L_0 = 2aN^{1/2}$. The dashed curves denote the well-studied flat brush (i.e., $R \rightarrow \infty$) results of SCFT and SST. The SST prediction for $\phi_1(r)$ is a parabola with a sharp cutoff at $r - R = L_0$; the SCFT profile has the same shape at intermediate r , but also includes a depletion region of width $\mu \sim L_0^{-1}$ next to the substrate and a tail of length $\xi \sim L_0^{-1/3}$ extending beyond the classical cutoff.⁷ For finite particles of $R/aN^{1/2} = 16, 4, 2, 1$, and 0.5 , the brush thickness decreases in accord with the simple SST predictions of $L_B/aN^{1/2} = 1.94, 1.80, 1.66, 1.47$, and 1.25 from eq 29, obtained by ignoring the existence of an exclusion zone. With a full proper SST treatment,²⁶ a region should develop next to the substrate where $g_1(r) = 0$, and as that happens $\phi_1(r)$ should deviate from the standard parabolic shape. Although the curves in Figure 3a become nonparabolic for $R \lesssim 2aN^{1/2}$, an exclusion zone is not evident in Figure 3b, even for the smallest particle of $R = 0.5aN^{1/2}$. Evidently, the brush is not sufficiently stretched (i.e., $L_0/aN^{1/2}$ is too small) for SST to be an accurate approximation of SCFT.

Figure 4 shows a similar series of profiles to those of Figure 3, but for an increasing solvent quality at a fixed particle size of $R = 2aN^{1/2}$. The parameter, Λ , is adjusted so that $L_0/aN^{1/2} = 1, 2, 4$ and 8 , which correspond to SST thicknesses of $L_B/aN^{1/2} = 0.90, 1.66, 2.94$ and 4.99 , respectively. Although this increase is consistent with the SCFT profiles, the actual extension of the brush is seriously underestimated by the SST values of L_B , until the chains become extremely stretched. At our highest value of $L_0 = 8aN^{1/2}$, the SCFT begins to match the SST predictions.²⁶ A significant exclusion zone in $g_1(r)$ now extends up to $r - R \approx 1.5aN^{1/2}$, at which point the shape of $\phi_1(r)$ switches from concave to convex. Realistically speaking,

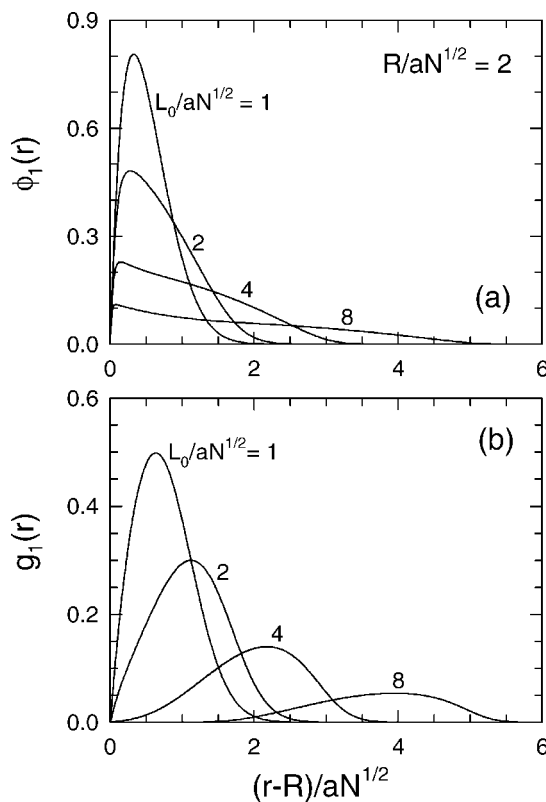


Figure 4. Analogous plots to those of Figure 3, but for a fixed particle radius, $R = 2aN^{1/2}$, and a series of Λ corresponding to selected values of $L_0/aN^{1/2}$.

however, this level of chain stretching is well beyond typical experimental conditions.⁷

Next we examine the compression of two particles of $R = 2aN^{1/2}$ separated by $2L = 2aN^{1/2}$ in a good solvent corresponding to $L_0 = 2aN^{1/2}$. Parts a and b of Figure 5 show contour plots of the single-brush segment profile, $\phi_1(\mathbf{r})$, and the combined profile, $\phi(\mathbf{r}) \equiv \phi_1(\mathbf{r}) + \phi_2(\mathbf{r})$, respectively. From the SST brush height of $L_B = 1.66aN^{1/2}$, we would expect a contact area extending to $\theta_c = 0.59 = 34^\circ$ (defined by $l(\theta_c) = L_B$). Because the SCFT profile extends somewhat beyond the SST prediction, the contact area also extends a little further to $\theta_c \approx \pi/4 = 45^\circ$. Despite the large contact area between the brushes, the segment profile, $\phi_1(r, \theta)$, quickly relaxes to its unperturbed shape in Figures 3a and 4a for $\theta \gtrsim \theta_c$. However, the perturbation to the end-segment distribution, $g_1(r, \theta)$, extends to significantly larger angles as illustrated in Figure 5c. This lateral displacement of segments is an indication that these particles are too small for the Derjaguin approximation.

For a more quantitative measure of the lateral displacement of segments, Figure 6 compares the profiles in the $\theta = 0$ and π directions. If there is no lateral displacement, then the compression will cause $\phi_1(r, 0)$ to increase above $\phi_1(r, \pi)$ such that the integrated number of segments, $\int dr r^2 \phi_1(r, \theta)$, remains fixed for all θ . Although the compression causes an increase in $\phi_1(r, 0)$ next to the particle, the integrated number of segments in the $\theta = 0$ direction drops by 29%. A similar calculation for $g_1(r, 0)$ shows that 39% of the end segments are displaced from the forward direction. Thus the key assumption of the Derjaguin approximation is indeed violated.

It is interesting to compare the profiles in Figure 6a with what we would expect from the simple SST treatment in the Appendix for uniform compression. If we can assume that the chain ends exist everywhere (i.e., no exclusion zone), then the field and hence the concentration will be parabolic. Thus as the brush is compressed, the profile must increase by an additive constant

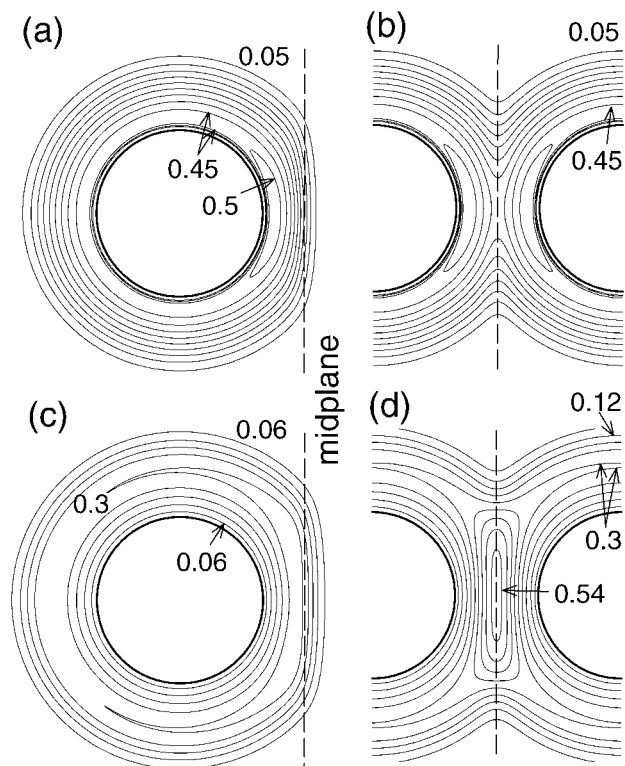


Figure 5. Contour plots of (a) $\phi_1(\mathbf{r})$, (b) $\phi(\mathbf{r}) \equiv \phi_1(\mathbf{r}) + \phi_2(\mathbf{r})$, (c) $g_1(\mathbf{r})$, and (d) $g(\mathbf{r}) \equiv g_1(\mathbf{r}) + g_2(\mathbf{r})$ calculated for two particles of radius $R = 2aN^{1/2}$, separated by a distance of $2L = 2aN^{1/2}$, and with Λ corresponding to $L_0 = 2aN^{1/2}$.

so as to maintain the required parabolic shape. Although this does not generally extend to nonuniform compression, it does apply to the two special cases of $\theta = 0$ and π , where by symmetry the classical (i.e., lowest-energy) trajectories follow the radial direction. Indeed the SCFT profiles in Figure 6a follow the parabolic shape reasonably well, provided the comparison in the forward direction is applied to the total concentration, $\phi(r, 0) \equiv \phi_1(r, 0) + \phi_2(r, 0)$. However, SST predicts zero interpenetration between the two brushes (i.e., neither brush crosses the midplane), and thus the parabolic profile should also apply to $\phi_1(r, 0)$. The fact that it does not indicates that L_0 is too small for SST to be completely reliable. Indeed, detailed comparisons with SCFT for flat brushes⁷ have shown that SST is generally inaccurate until $L_0 \gtrsim 10aN^{1/2}$.

Now we turn our attention to the interaction potential, $\Delta F(L; R)$. Figure 7a shows $\Delta F(L; R)$ as a function of compression, L , for the different particle radii, R , considered in Figure 3, while Figure 7b shows analogous plots for the different values of L_0 considered in Figure 4. The onset of the interaction is expected to coincide with the respective points in Figures 3a and 4a where $\phi_1(r)$ acquires an appreciable value (e.g., $\phi_1(r) \sim 10^{-2}$). As it happens, the outer part of the brush is extremely soft and thus there is considerable interpenetration before any significant interaction is observed. Nevertheless, in each and every case, the interaction energy strictly increases with compression, in stark contrast to the attraction predicted previously by Roan¹³ under similar conditions.

So far, we have assumed that the chain ends are chemically bonded to the particles such that the grafting points remain uniformly distributed over the particle surface (i.e., $\sigma(\theta) = \text{constant}$). However, when the ends are instead physically adsorbed, they can diffuse along the grafting surface away from the crowded region between the particles so as to lower the free energy. Figure 8a shows the reduced energy penalty of the physically adsorbed brush, eq 20, compared to that of the

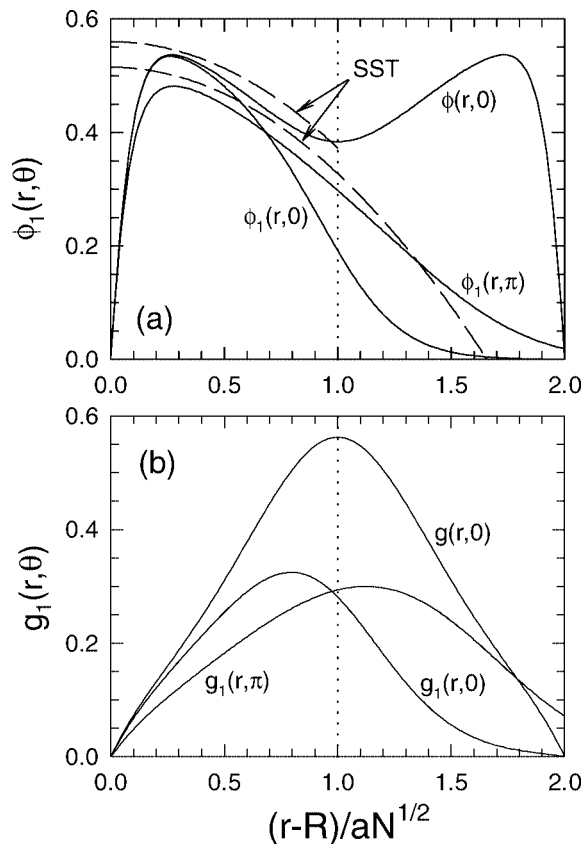


Figure 6. (a) Total segment and (b) end-segment concentrations from Figure 5 plotted in the $\theta = 0$ and π directions. The dotted line denotes the midplane for $\theta = 0$, and the dashed curves denote SST predictions for $\phi_1(r, \theta)$.

chemically bonded brush, eq 18. Although the two interaction potentials start off nearly the same, a significant difference does develop at high compressions. Figure 8b confirms that this feature is the result of chain end movement. It is interesting to note that the depletion of chain ends coincides reasonably well with the contact region (i.e., $\theta \lesssim \theta_c$), beyond which the grafting density reaches a plateau. Naturally, the plateau level is slightly higher than the average grafting density, σ , so as to compensate for the depletion at small angles.

The dashed curves in Figure 7a denote the standard Derjaguin approximation in eq 25, calculated numerically with SCFT and analytically with SST (see eq 31). The considerable discrepancy between the SCFT and SST curves is a further indication that $L_0 = 2aN^{1/2}$ is too small for the application of SST. Nevertheless, the exact SCFT results (solid curves) do converge to the SCFT-based Derjaguin approximation (upper dashed curve), although very large particles (e.g., $R \gtrsim 10L_0$) are required before the approximation can be considered as reasonably accurate. This is the same conclusion reached by the previous studies in refs 4 and 10. Fortunately, there exists an improved version.

Figure 9 examines the improved Derjaguin approximation from eq 22 for several conditions where $R \lesssim L_0$. The Derjaguin approximation (dashed curve) still overestimates the actual interaction (solid curve), but now the agreement is quite good for modest compressions. Again the approximation is compared to calculations for chemically bonded polymers (i.e., $\sigma(\theta) = \text{constant}$); naturally, the agreement will be slightly reduced for physically adsorbed chains since the actual interaction will decrease while the Derjaguin approximation will remain unchanged. Nevertheless, this is not much of an issue since the Derjaguin approximation begins to fail at about the same point where the bonded and adsorbed brushes start behaving differ-

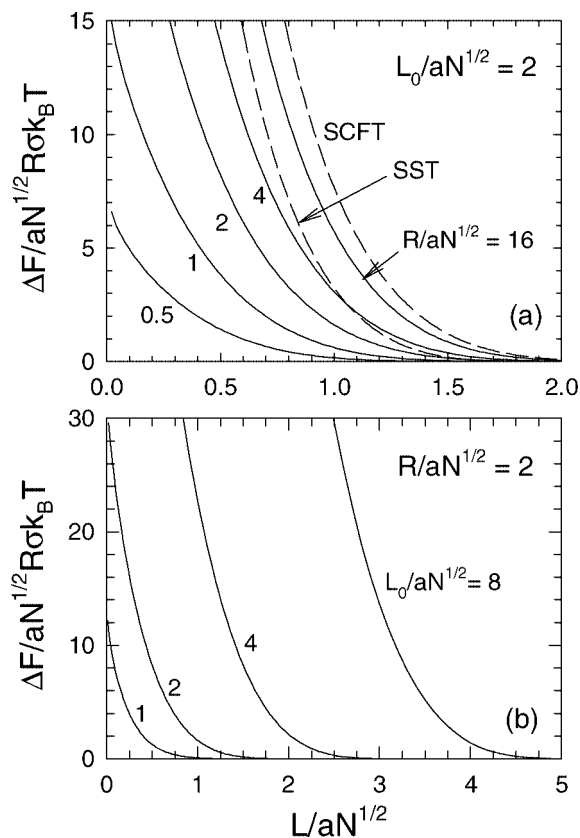


Figure 7. Interparticle potential, $\Delta F(L; R)$, as a function of separation, L , plotted for (a) the same sequence of particle radii examined in Figure 3 and (b) the sequence of brush thicknesses considered in Figure 4. The two dashed curves in the upper plot denote the standard Derjaguin approximation in eq 25 as calculated by SCFT and SST.

ently. We have also included analogous SST predictions in Figure 9, using the method described in ref 4. Just as before, the SST proves to be rather inaccurate for $L_0 = 2aN^{1/2}$, but it does much better for $L_0 = 4aN^{1/2}$.

Discussion

We have developed an accurate and efficient SCFT algorithm for examining the interaction between two polymer-grafted spherical particles, but it is nevertheless limited to certain assumptions.⁷ For example, its use of course-grained Gaussian chains assumes high molecular weights. The grafting density must also be large, because the initial condition for $q_g(\mathbf{r}, s)$ in eq 17 neglects the discreteness of the grafting distribution. Furthermore, the implementation of mean-field theory also requires a sufficient polymer concentration such that the screening distance for excluded-volume interactions (i.e., the blob size²⁷) is small, but neither can the concentration be too high because the self-consistent field, eq 6, includes a contribution from the translational entropy of the *implicit* solvent obtained by expanding to second order in $\phi(\mathbf{r})$.²⁷ Thus, the solvent quality has to be good but not too good, so that the brushes remain in the semidilute regime. However, the SCFT does not require the polymers to be strongly stretched as in the SST. Although these conditions may seem somewhat restrictive, they are well satisfied by the new polymer-coated nanoparticles created by *grafting-to* techniques.²⁸ If necessary, many of the assumptions can actually be removed with simple extensions to the SCFT.⁷

Part of our motivation for this work was the previous SCFT calculations of Roan and Kawakatsu,^{3,12,13,20} which predicted $\Delta F(L; R) < 0$ for small values of R and L_0 . This result

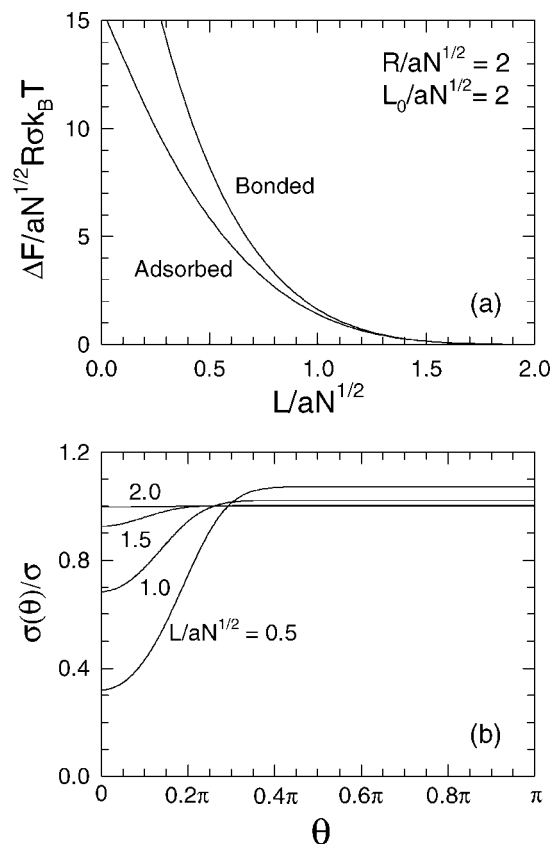


Figure 8. (a) Comparison of the interparticle potential, $\Delta F(L; R)$, for chemically bonded brushes (i.e., constant $\sigma(\theta)$) and physically adsorbed brushes calculated for a particle radius of $R = 2aN^{1/2}$ and a Λ corresponding to $L_0 = 2aN^{1/2}$. (b) Equilibrium grafting density, $\sigma(\theta)$, of the physically adsorbed brushes at various levels of compression, L .

contradicts a simple mean-field argument in ref 17, which implies that the free energy of a given particle cannot decrease with the introduction of a second particle (assuming no direct particle–particle interaction such as the van der Waals attraction). Although our present calculation agrees with this strict constraint that $\Delta F(L; R) \geq 0$ under all conditions, it begs the question of why the previous calculations did not.

Naturally, numerical inaccuracy is one likely factor contributing to the erroneous attraction. This is because the bispherical coordinate system used by Roan and Kawakatsu results in a very uneven mesh; the grid spacing tends to be particularly sparse on the backside of the two spheres (i.e., $\theta = \pi$), and this problem is greatly exacerbated as $L \rightarrow 0$. Not only did they have to cope with the serious numerical inefficiency of a nonuniform mesh but also their numerical inaccuracy would have had a strong L dependence, which may have manifested itself as an attraction. By contrast, our algorithm is much more efficient since the spherical–polar coordinate systems provide relatively uniform meshes, and our numerical inaccuracy is much easier to control because the grid spacing remains fixed.

There is another very subtle problem with the bispherical coordinate system involving the separation, ε , between the particle and the grafting surface, which is necessary so that the initial condition for $q_g(\mathbf{r}, s)$ does not violate the Dirichlet boundary condition. As long as ε is chosen to be small (e.g., one grid spacing), the finite separation has a negligible effect on most quantities such as the segment concentrations. However, since the earlier calculations of Roan and Kawakatsu, it has been shown⁷ that there is a divergence in the free energy that scales as $\ln \varepsilon$. It is an unphysical consequence of placing infinitely flexible Gaussian chains next to an impenetrable

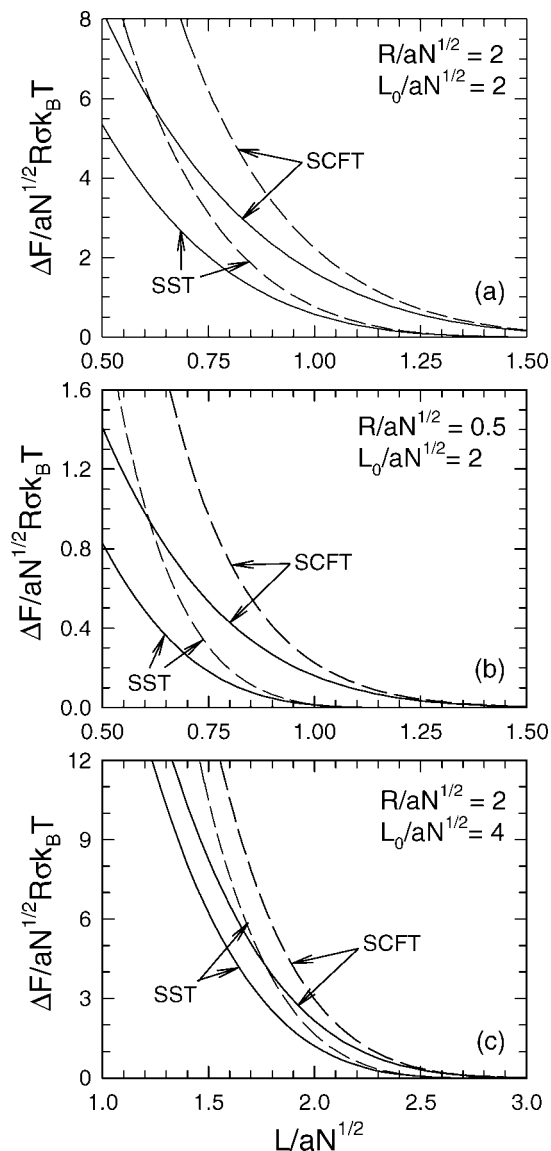


Figure 9. Comparison of the interparticle interaction energy (solid curve) with the Derjaguin approximation in eq 22 (dashed curve) for several combinations of particle radius, R , and brush extension, L_0 . Curves are calculated by the present SCFT method and the previous SST algorithm in ref 4.

surface. Nevertheless, the divergence has no effect on the free energy difference, $\Delta F(L; R)$, provided that ϵ remains constant, which is the case in our calculation. In the calculation of Roan and Kawakatsu, however, the mesh and thus ϵ changes with L , resulting in an unphysical contribution to $\Delta F(L; R)$.

The strong energy dependence on the separation between the grafted ends and the particle surface could also be an issue in the SCFT calculation of Wijmans and co-workers.¹⁰ Their use of a cylindrical coordinate system made it impossible to graft the chains a uniform distance, ϵ , from the spherical particles. Therefore, they grafted the chain ends in a narrow band above the particles with an appropriate weighting for each lattice site in order to achieve a reasonably uniform grafting density. Although it is impossible to know for certain, we suspect that they probably moved the spheres in integer intervals of the grid spacing, such that there was no variation in the grafting distribution relative to the particle surface. If so, they would have avoided the problem that plagued the SCFT calculations of Roan and Kawakatsu. Indeed, they reported only repulsive interactions.

In the Theory section, we obtained the polymer concentration of the second particle, $\phi_2(\mathbf{r})$, by reflecting that of the first particle (see eq 9). Thus, at first glance, it may appear that the previous approaches using cylindrical¹⁰ or bispherical¹⁵ coordinates are more versatile, since they allow for particles of different sizes and/or different brush properties. In fact, the generalization of our multicoordinate-system (MCS) scheme is extremely versatile. If particle two is different from one, then the field is simply transformed to the second coordinate system, $\bar{\mathbf{r}}$, and $\phi_2(\bar{\mathbf{r}})$ is then calculated in those coordinates. If there are three particles, then we just define another spherical–polar coordinate system centered on the third particle; of course, we would then lose the azimuthal symmetry (i.e., the invariance in φ), but our procedure is sufficiently efficient that the calculation would still remain feasible. Likewise, the MCS scheme can be applied to differently shaped objects such as two cylindrical rods, or a spherical particle interacting with a planar surface. It is just a simple matter of choosing the appropriate coordinate system for each object.

In Figure 8, we considered the compression of physically adsorbed brushes and the resulting rearrangement, $\sigma(\theta)$, of the grafted chain ends. The calculation is based on an assumption that each chain is attached by a functional end, which is free to move along the surface of the particle but is unable to detach. This requires that the two particles stay in contact long enough for $\sigma(\theta)$ to adopt an equilibrium distribution. If the time of contact is not sufficient, the force will likely be something intermediate to the two curves in Figure 8. In principle, we could also allow the chains to detach, in which case there would have to be a small population of free chains in the solvent background, with some specified chemical potential. In addition to this extra parameter, the model would also have to specify an adsorption energy. In this latter case, however, it is even more doubtful that an equilibrium treatment would be valid.

Here we found that the SST seriously underestimates the SCFT predictions, although the difference is significantly diminished for the thicker brushes considered in Figure 9c. This underestimation can largely be attributed to the fact that the SCFT distribution, $\phi_1(r)$, of the isolated particle extends well beyond the thickness L_B predicted by SST (see Figures 3 and 4 and related text). Consequently, the SST misjudges the onset of the interaction. It should also be noted that the true difference between SCFT and SST may not be as large as portrayed in Figure 9, because the SST results referred to in this paper have been supplemented by a couple of approximations in addition to the strong-stretching assumption. First of all, they ignore the exclusion zone near the substrate, which becomes increasingly important as R/L_0 decreases.²⁶ Second of all, the SST calculation for nonuniform compression in Figure 9 allows the chains to tilt (or splay) away from the $\theta = 0$ direction, but does not allow them to bend. In any case, the true accuracy of SST is a rather academic issue, since the full SST calculation accounting for exclusion zones and curved trajectories would actually be more complicated than our SCFT calculation.

The conventional Derjaguin approximation in eq 25 based on the uniform compression of a flat brush is derived under the assumption that $R \gg L_0$, and indeed we found that it only works well for large particles of $R \gtrsim 10L_0$. The biggest source of inaccuracy originates from the reduction in the brush thickness (i.e., L_B) that occurs for curved substrates, and consequently, eq 25 overestimates the range of the interaction. This shortcoming is easily remedied by the improved Derjaguin approximation in eq 24, where the interaction, $\Delta F(L; R)$, is estimated from the uniform compression of a curved brush. In this way, the approximation predicts the correct onset of the interaction and remains accurate for small compressions of $L_B - L \ll R + L_B$. With this simple modification, the Derjaguin approximation

remains applicable for particles smaller than even L_0 (see Figure 9). Furthermore, there is no real cost for this improvement, since the SCFT for the uniform compression of a curved brush is equally trivial to that of a flat brush. However, as a word of caution, our results in Figures 5 and 6 as well as past experience^{4,19} demonstrates that the Derjaguin approximation is not so successful at predicting segment distributions. Not only that, it can only be applied to identical particles, where the symmetry allows one to define $l(\theta)$ (see Figure 2). Thus even the improved Derjaguin approximation could never completely substitute the full SCFT treatment.

Conclusion

The interaction energy, $\Delta F(L; R)$, between polymer-grafted particles in good solvent (see Figure 1) has been calculated using self-consistent field theory (SCFT). Contrary to the attraction predicted previously,^{3,12,13,20} we found that the interaction is strictly repulsive regardless of the particle separation L , particle radius R , or brush thickness L_0 . The erroneous attraction of the previous SCFT calculations is attributed to difficulties associated with the use of bispherical coordinates, involving numerical inaccuracy as well as a subtle problem in the way chains are attached to the particles. Here, we overcome these difficulties by using a multicoordinate-system (MCS) scheme, where separate sets of spherical-polar coordinates are defined about the two particle centers (see Figure 2). This new MCS scheme produces a computationally efficient algorithm with negligible numerical inaccuracies and a high degree of versatility.

The accurate predictions of our full SCFT calculation were also used to test previous approximations. The simplified SST calculation in ref 4 produces a very similar interaction potential, except that it underestimates the range of the interaction by a substantial margin. The standard Derjaguin approximation^{10,24} in eq 25 produces reliable predictions, but only for large particles (e.g., $R \gtrsim 10L_0$). On the other hand, the improved Derjaguin approximation^{4,23} in eq 24 works for very small particles, provided that the brush does not become too compressed.

Acknowledgment. We thank Alberto Striolo for clarifying some details regarding ref 8 and the EPSRC for financial support (Grant No. EP/D031494/1).

Appendix: SST for Uniform Compression

Here we briefly introduce an approximate solution to the strong-stretching theory (SST) for the uniform compression of an isolated spherical brush. In this limit, the chains follow radial trajectories, $r_\alpha(s)$, perpendicular to the particle surface. According to the classical argument by Milner et al.,⁶ the field must be harmonic

$$w(r) = \frac{3\pi^2(C - (r - R)^2)}{8a^2N} \quad (27)$$

so that the corresponding chain trajectories

$$r_\alpha(s) = R + (r_0 - R) \cos(\pi s/2) \quad (28)$$

reach the substrate (e.g., $r_\alpha(1) = R$) in one unit of s regardless of the positions of their free ends (e.g., $r_\alpha(0) = r_0$). In reality, the argument does not hold for curved surfaces, because there is in fact an exclusion zone near the substrate where $g_1(r) = 0$.²⁶ Nevertheless, the parabolic potential remains reasonably accurate, provided that the curvature is not too high.

Once the field is known, the concentration, $\phi_1(r) = w(r)/\Lambda$, follows directly from eq 6. The constant, C , in eq 27 is then determined by the normalization of $\phi_1(r)$ in eq 5. Furthermore,

the fact that $\phi_1(r)$ must remain positive sets a lower limit of $C = L_B^2$, where L_B defines the height of an unperturbed brush determined by

$$\frac{L_B}{L_0} = \left(1 + \frac{3L_B}{4R} + \frac{L_B^2}{5R^2}\right)^{-1/3} \quad (29)$$

When the brush is uniformly compressed to a height of $l < L_B$, the constant increases to

$$C = \frac{20R^2L_0^3 + 6l^5 + 15l^4R + 10l^3R^2}{10l^3 + 30l^2R + 30lR^2} \quad (30)$$

The free energy per chain is then given by

$$\frac{f(l; R)}{k_B T} = \frac{3\pi^2 C}{8a^2 N} - \frac{1}{2R^2 a N^{1/2}} \int_R^{R+l} dr r^2 w(r) \phi_1(r) \quad (31)$$

where the first term is the average of $E[r_\alpha]$ from eq 2 and the second term corrects for the usual double counting of the internal energy by mean-field theory. For an uncompressed brush (i.e., $l \geq L_B = \sqrt{C}$), the free energy is given by the simple expression

$$\frac{f(L_B; R)}{k_B T} = \frac{9\pi^2 L_B^5}{40a N^{1/2} L_0^3} \left(1 + \frac{5L_B}{6R} + \frac{5L_B^2}{21R^2}\right) \quad (32)$$

The expression for a compressed brush (i.e., $l < L_B$) is analytical but rather messy, and consequentially the integral for the Derjaguin approximation in eq 24 has to be performed numerically. However, in the $R \rightarrow \infty$ limit, things simplify sufficiently that the integral for the standard Derjaguin approximation in eq 25 can be performed analytically to give

$$\frac{\Delta F(L; R)}{k_B T} = \frac{9\pi^3 \sigma R L_0^3}{20a^2 N} H(L/L_0) \quad (33)$$

where

$$H(u) \equiv (-45 - 30 \ln u + 54u - 10u^3 + u^6)/54 \quad (34)$$

for $u \leq 1$ and is zero otherwise.

References and Notes

- (1) (a) Napper, D. H. *Polymeric Stabilisation of Colloidal Dispersions*; Academic Press: London, 1983. (b) Russel, W. B.; Saville, D. A.; Schowalter, W. R. *Colloidal Dispersions*; Cambridge University Press: Cambridge, U.K., 1989.
- (2) Derjaguin, B. V. *Kolloid Z.* **1934**, *69*, 155.
- (3) Roan, J.-R. *Int. J. Mod. Phys. B* **2002**, *17*, 2791.
- (4) Matsen, M. W. *Macromolecules* **2005**, *38*, 4525.
- (5) Semenov, A. E. *JETP* **1985**, *61*, 733.
- (6) (a) Milner, S. T.; Witten, T. A.; Cates, M. E. *Europhys. Lett.* **1988**, *5*, 413. (b) Milner, S. T.; Witten, T. A.; Cates, M. E. *Macromolecules* **1988**, *21*, 2610.
- (7) Kim, J. U.; Matsen, M. W. *Eur. Phys. J. E* **2007**, *23*, 135.
- (8) (a) Striolo, A. *Phys. Rev. E* **2006**, *74*, 041401. (b) Striolo, A.; Egorov, S. A. *J. Chem. Phys.* **2007**, *126*, 014902.
- (9) (a) Cerda, J. J.; Sintes, T.; Toral, R. *Macromolecules* **2003**, *36*, 1407. (b) Tej, K.; Meredith, J. C. *J. Chem. Theory. Comput.* **2006**, *2*, 1624. (c) Duque, D.; Peterson, B. K.; Vega, L. F. *J. Phys. Chem.* **2007**, *111*, 12328.
- (10) Wijmans, C. M.; Leermakers, F. A. M.; Fleer, G. J. *Langmuir* **1994**, *10*, 4514.
- (11) Scheutjens, J. M. H. H.; Fleer, G. J. *J. Phys. Chem.* **1979**, *83*, 1619.
- (12) Roan, J. *Phys. Rev. Lett.* **2001**, *86*, 1027.
- (13) Roan, J. *Phys. Rev. Lett.* **2001**, *87*, 059902.
- (14) Edwards, S. F. *Proc. Phys. Soc. London* **1965**, *85*, 613.
- (15) Roan, J.; Kawakatsu, T. *J. Chem. Phys.* **2002**, *116*, 7283.
- (16) Bhatia, S. R.; Russel, W. B. *Macromolecules* **2000**, *33*, 5713.
- (17) Matsen, M. W. *Phys. Rev. Lett.* **2005**, *95*, 069801.
- (18) Matsen, M. W. In *Soft Matter*; Gompper, G., Schick, M., Eds.; Wiley-VCH: Weinheim, Germany, 2006; Vol. 1; Chapter 2.
- (19) Kim, J. U.; Matsen, M. W. *Macromolecules* **2008**, *41*, 246.
- (20) Roan, J.; Kawakatsu, T. *J. Chem. Phys.* **2002**, *116*, 7295.
- (21) Press, W. H.; Teukolsky, S. A.; Vetterling, W. T. *Numerical Recipes in C: the Art of Scientific Computing*; Cambridge University Press:

- Cambridge, U.K., 1993.
- (22) Thompson, R. B.; Rasmussen, K. Ø.; Lookman, T. J. *Chem. Phys.* **2004**, *120*, 31.
- (23) Nommensen, P. A.; Duits, M. H. G.; van den Ende, D.; Mellema, J. *Langmuir* **2000**, *16*, 1902.
- (24) (a) Mewis, J.; Frith, W. J.; Strivens, T. A.; Russel, W. B. *AIChE J.* **1989**, *35*, 415. (b) Borukhov, I.; Leibler, L. *Phys. Rev. E* **2000**, *62*, R41.
- (25) (a) Dan, N.; Tirrell, M. *Macromolecules* **1992**, *25*, 2890. (b) Wijmans, C. M.; Zhulina, E. B. *Macromolecules* **1993**, *26*, 7214.
- (26) Li, H.; Witten, T. A. *Macromolecules* **1994**, *27*, 449.
- (27) de Gennes, P.-G. *Scaling Concepts in Polymer Science*; Cornell University Press: Ithaca, NY, 1979.
- (28) (a) Pyun, J.; Kowalewski, T.; Matyjaszewski, K. *Macromol. Rapid Commun.* **2003**, *24*, 1043. (b) Pyun, J.; Jia, S.; Kowalewski, T.; Patterson, G. D.; Matyjaszewski, K. *Macromolecules* **2003**, *36*, 5094. (c) Bombalski, L.; Dong, H.; Listak, J.; Matyjaszewski, K.; Bockstaller, M. R. *Adv. Mater.* **2007**, *19*, 4486.

MA8002856